Applied Geomatics (2026) 18:24
https://doi.org/10.1007/s12518-025-00675-x

RESEARCH

# Study on the accuracy of Multi-GNSS PPP for different observing sessions time spans using PRIDE PPP-AR open-source software package

**Matteo Cappuccio[1] · Luca Tavasci[1] · Luca Poluzzi[1] · Stefano Gandolfi[1]**

Received: 11 July 2025 / Accepted: 19 November 2025



## Abstract

The Precise Point Positioning (PPP) approach to GNSS observables is widely used for processing data from permanent stations, providing highly precise coordinates. However, the performance of PPP for observation sessions shorter than 24 h has not yet been thoroughly investigated in the case of multi-constellation acquisitions. In recent years, the PRIDE PPP-AR software package has been made freely available. Since it includes a graphical user interface (GUI) version that runs under Windows, it can also be easily used by technical surveyors aiming to process data acquired from a single GNSS receiver. This is particularly valuable for surveys conducted in areas lacking dense geodetic infrastructures or reliable augmentation services. In this paper, based on a wide and consistent dataset, the coordinate precision obtained from observation sessions ranging from 30 min to 24 h processed with PRIDE PPP-AR is analyzed. In addition to multi-constellation GNSS data (GPS + Galileo + GLONASS + BeiDou), independent GPS-only and Galileo-only processing was also evaluated. Furthermore, the reliability of the formal errors provided by the software was examined, as these represent the only available information for assessing coordinate quality in surveys that lack geometric redundancy. While several online PPP services already exist, PRIDE PPP-AR overcomes common limitations related to the number of processed files and the choice of GNSS constellations. The results show that two-hour observation sessions can reliably achieve horizontal coordinate accuracy within 2 cm and vertical accuracy within 5 cm, whereas 30-minute sessions are suitable for applications requiring 5–10 cm accuracy.


**Keywords** GNSS · Precise point positioning · PRIDE PPP-AR · Galileo · Network densification · Static surveying

## Introduction

The Precise Point Positioning (PPP) approach for processing GNSS observations is nowadays widely used and implemented in several software packages. Its strength lies in the capability to provide precise coordinates of a stand-alone receiver, thus avoiding the computational burden of managing a baseline network. PPP has become a standard technique in geodesy (An et al. 2020; Kouba et al. 2017; Zumberge et al. 1997), Earth sciences, and particularly in atmospheric studies using GNSS (Yang et al. 2023; Zhu et al. 2023). The approach was first implemented in the GIPSY-OASIS software package (Webb and Zumberge 1997) by the Jet Propulsion Laboratory (JPL). With release 6.1, ambiguity resolution was introduced (Bertiger et al. 2010), further enhancing PPP performance. Among scientific software for GNSS data processing, the Bernese GNSS software package (Teferle et al. 2007) also introduced a PPP module in release 5.0 (Dach et al. 2015). Over the past decades, PPP applied to permanent GNSS stations has demonstrated coordinate repeatability comparable to, or even better than, the classical differenced approach—particularly in wide networks with very long baselines (Chu and Yang 2014; Li et al. 2014). To achieve optimal performance, PPP requires post-processed products such as ephemerides, clock biases, Earth Orientation Parameters (EOP), phase biases, and satellite attitude information. These products are currently provided

✉ Matteo Cappuccio
matteo.cappuccio@unibo.it

1 DICAM – University of Bologna, Viale del Risorgimento 2, Bologna 40136, Italy

Published online: 26 November 2025

by several analysis centers, including the International GNSS Service (IGS), JPL (https://gipsyx.jpl.nasa.gov/index.php?page=data), the Center for Orbit Determination in Europe (CODE), and Wuhan University (WHU) (Dach et al. 2024; Guo et al. 2016; Kouba and Héroux 2001). The unavailability of these precise products in real time, combined with the need for complex scientific software, has long discouraged surveyors from using PPP for technical applications. Moreover, due to its reduced redundancy of observations compared with the differenced approach, PPP suffers from long convergence times (Abou-Galala et al. 2018; Glaner And Weber 2021), making it unsuitable for rapid surveys. Nevertheless, PPP has also been employed for kinematic positioning in remote areas (Cappuccio et al. 2024), thanks to its independence from dense ground infrastructures. To enable real-time kinematic positioning in remote and offshore environments, several commercial PPP-based services have emerged, such as Starfix, C-Nav, Trimble RTX, and Atlas (Atiz et al. 2023; C-Nav Positioning Solutions n.d.; Naciri et al. 2023). These services provide real-time PPP corrections computed from wide-area CORS networks. Although they are usually expensive, they deliver reliable sub-decimeter positioning, with even centimeter-level pass-to-pass repeatability (Tavasci et al. 2021), suitable for offshore or agricultural applications but insufficient for more demanding tasks requiring higher accuracy. Indeed, some technical applications demand both centimeter-level absolute accuracy and the shortest possible static observation sessions. Examples include densification surveys of passive benchmarks realizing reference frames for monitoring or relative surveying techniques (RTK, total stations, laser scanners, etc.) (Tavasci et al. 2023; Vecchi et al. 2021). Long-term monitoring of remote areas (e.g., landslides or glaciers) where installing permanent GNSS stations is impractical also represents a context where PPP can be effectively applied using static sessions of a few hours over ground benchmarks.

In Gandolfi et al. (2017), an investigation into achievable PPP precision in such contexts demonstrated sub-centimeter coordinate repeatability with observation sessions of six hours or more, while precision significantly decreased for sessions shorter than one hour. Barbarella et al. (2018) further proposed a mathematical model linking PPP precision to session duration. Both studies relied solely on GPS data processed with GIPSY-OASIS II, a software not easily accessible to surveyors, thus limiting the practical use of their findings.

Over the years, several online PPP services have been developed, allowing users to upload RINEX (Receiver INdependent EXchange) files for processing, such as CSRS-PPP (Tetreault et al. 2005), GAPS (Leandro et al., 2007), magicPPP (https://www.gmv.com/en/products/space/magicppp), MADOCA (https://qzss.go.jp/en/overview/services/sv13_madoca.html) and APPS (http://apps.gdgps.net/). Most of these services use JPL software to perform PPP. While user-friendly, they do not allow large dataset processing, limiting robust performance assessments. Nevertheless, studies such as Vázquez-Ontiveros et al. (2023) and Mutlu et al. (2023) have provided insights into the precision achievable through such online platforms, although they typically relied on datasets covering only about seven days.

A more recent and comprehensive analysis of PPP performance as a function of both session duration and site latitude was conducted by Kurtz et al. (2024), using GPS data and the Parallel.GAMIT software (https://github.com/demiangomez/Parallel.GAMIT) However, this software requires customized Python scripting, which makes it less suitable for surveyors seeking user-friendly tools.

Recently, PPP has been implemented in several new software packages, such as GipsyX, Bernese v5.4, and PRIDE PPP-AR (Bertiger et al. 2020; Geng et al. 2019). Among these, PRIDE PPP-AR stands out for its intuitive graphical interface and full availability for public use, making it accessible to a wide range of surveyors, researchers, and institutions interested in PPP post-processing of static GNSS data. Unlike the previously used GIPSY-OASIS II, PRIDE PPP-AR supports full multi-constellation processing, thereby improving observation redundancy and potentially enhancing PPP performance, particularly for shorter observation sessions.

The aim of this paper is to provide the scientific and technical community with updated information on PPP precision as a function of the observation time over a benchmark. PRIDE PPP-AR was selected for this study because, at present, it is among the most accessible tools for both technical and scientific users due to its user-friendly GUI, which runs on Windows. Consistently, default GUI processing parameters were applied in all tests, which were executed using the Linux (scriptable) version of the software to allow the processing of a robust dataset of more than 3,300 daily files.

The dataset includes a cluster of nine stations distributed across various latitudes providing 30-second RINEX files, as well as three permanent Italian stations also providing 1 Hz data. The analyzed time spans range from 24 h down to 30 min. Precision was evaluated for full-constellation (GPS + Galileo + GLONASS + BeiDou), GPS-only, and Galileo-only datasets. Moreover, since geometric redundancy (i.e., multiple baselines converging on a single point) is not possible in PPP, the covariance matrix estimated by the software is the only available indicator of coordinate quality. Therefore, this paper also proposes a method to correctly interpret and exploit this information, together with an assessment of its reliability.

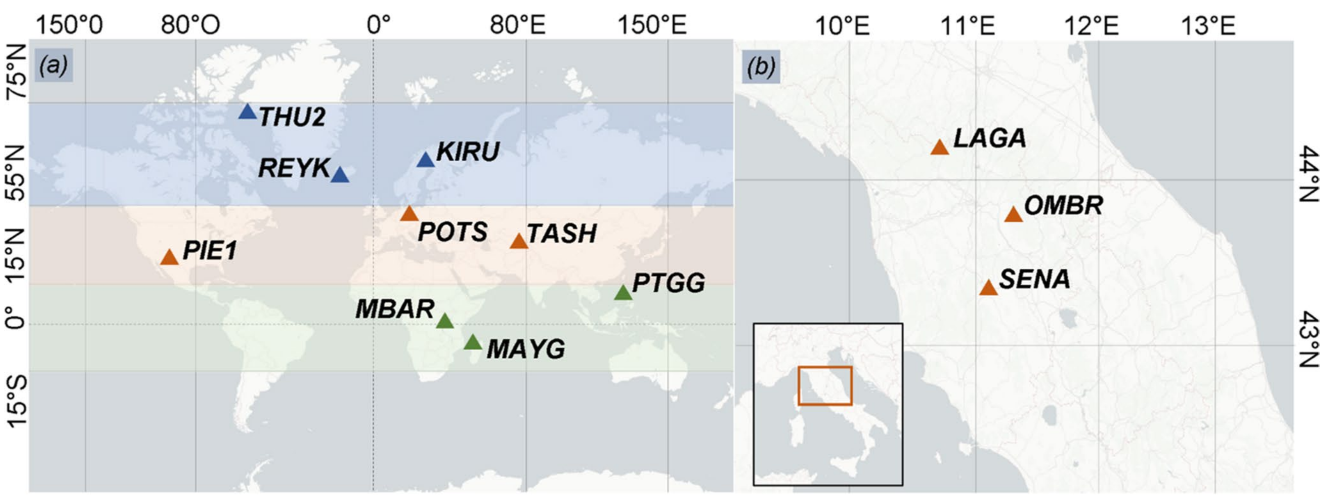


**Fig. 1** Maps showing the location of the 12 GNSS permanent stations providing the dataset, all equipped with full constellation receivers

**Table 1** Main products, models and parameters used in the PRIDE PPP-AR data processing

| Product | Source | File |
|---|---|---|
| *Orbits* | http://ftp.aiub.unibe.ch/CODE_MGEX/CODE/2023/ | COD0MGXFIN*05 M*.SP3 |
| *Clock* | | COD0MGXFIN*30S*.CLK |
| *Bias* | | COD0MGXPSFIN*.BIA |
| *Sat. Attitude* | | COD0MGXFIN*30S*.OBX |
| *Rec. antenna calibration* | https://files.igs.org/pub/station/general/ | Igs20.atx |
| *Sat. antenna calibration* | | |
| *Phase center mass correction* | | |
| | ***Model*** | |
| *EOP, Solid and Pole Tides* | IERS 2010 conventions (Technical note 36), Chap. 7 | |
| *OceanLoad model* | FES2014b | |
| *Tropospheric mapping function* | VMF-1 | |
| *Parameter* | ***Value*** | |
| *Elevation mask* | 10° | |
| *Carrier signal* | L1(E1)-L2-E5(a) | |

## Dataset and GNSS data processing

To perform the test, data from 12 GNSS permanent stations, all equipped with full constellation receivers, were used. In particular, a one-year dataset was acquired from 9 IGS stations located at three different latitude bands, as shown in Fig. 1a. These provided 30 s sampling rate RINEX files. Besides the 24 h, the following time spans were considered: 12 h, 6 h, 3 h, 2 h, 1 h and 0.5 h. Each daily file was split into several shorter one so that, for instance, 24 independent PPP solutions were obtained from 1 h observing sessions.

To test the impact of a higher rate of acquisition, also 30 days of 1 Hz observations were acquired from 3 stations belonging to a local monitoring network located in Italy as shown in Fig. 1b. For this dataset, only the 3 h, 2 h, 1 h and 0.5 h time spans were computed besides the daily ones. Both 1 Hz and 30 s sampled data were processed to assess the influence of the sampling rate on coordinate repeatability under identical hardware and environmental conditions. In the paper, multi-constellation solutions refer to all the four GNSS operative at the time. Moreover, for the time spans of 3 h and less, also the solutions given independently by the GPS and the Galileo constellations were computed respectively.

As for the data processing, it was carried out using the PRIDE PPP-AR software installed in a Linux environment and executed through ad hoc scripts to speed it up considering the amount of involved data. The main processing setting and products necessary to enable ambiguity resolution are listed in Table 1. These are nothing but the default parameter, also implemented in the GUI version which non expert users would use. The only exception concerns the orbit products: in the test we used the CODE ones for our convenience, while using the GUI the WHU products are automatically downloaded. Both set of products enable PPP

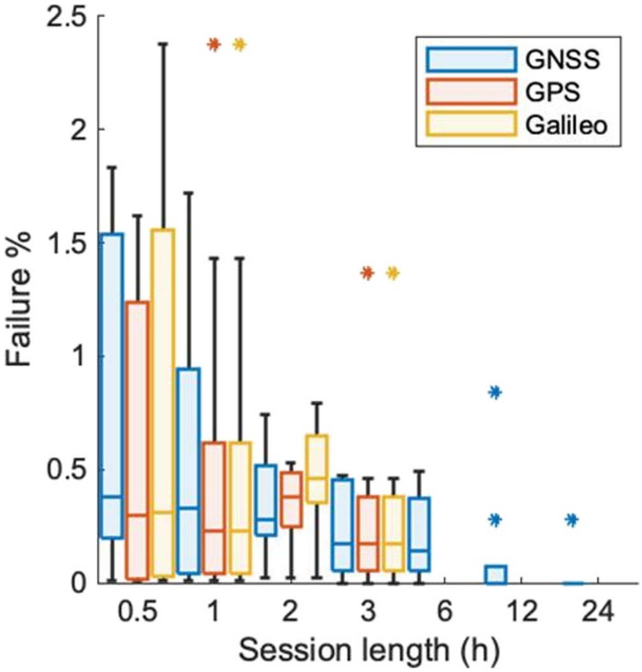


**Fig. 2** Boxplot reporting the statistics on the processing failure percentages over the 9 GNSS station from the IGS network. Boxes indicate interquartile ranges, whiskers represent extreme values, and asterisks denote outliers. GNSS results refer to full-constellations data

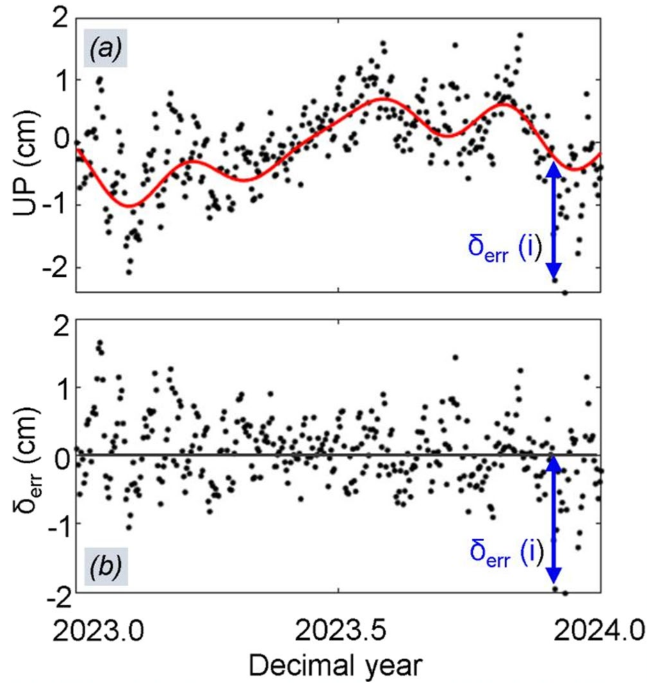


**Fig. 3** Example of one year positions time series (black dots), reference position model (red line), and residual coordinate representing the real error $\delta_{err}$

ambiguity resolution and switching from one to the other should not have a significant impact on the results.

As for the ambiguity resolution, PRIDE PPP-AR implements two different algorithms: the Lambda (JONGEPDE & TIBERIUSC, 1996) and the Rounding one (Jianghui Geng et al. 2010). The first is recommended for observing sessions shorter than 6 h, while the Rounding approach is preferred for longer data acquisitions. The GUI version of the software automatically switch between the two depending on the input data.

The PPP computations over data spans shorter than 24 h were obtained by using the "starttime and endtime" option in the PRIDE PPP-AR software, thus easily enabling the independent processing of the selected observations without the need to split each RINEX file into shorter files. Figure 2 reports the processing failure rate, namely the lack of coordinate in the output, depending on the site and the considered time span. As shown, the PPP processing has an increasing failure rate for shorter observing sessions, still under the 2.4% even the worst cases.

For each PPP solutions, PRIDE PPP-AR provides the ECEF site coordinates, together with the full cofactors matrix. Before proceeding with the analysis, both the coordinates and their estimated uncertainties were reprojected using topocentric systems along the East, North and Up (ENU) to split the plane directions from the vertical one.

## Analysis methods

The post-processing of the PPP solutions aimed to compute their "real error", defined as the difference between the estimated coordinates and corresponding reference values, in order to build statistics describing how such errors vary with observation duration.

The first step involved defining a reference position for each selected station. This reference was obtained from the 24-hour multi-constellation solutions by fitting nonlinear position models (Fig. 3a), as previously done in Gandolfi et al. (2017). The Lomb–Scargle periodogram (Scargle 1982; VanderPlas 2018) was applied to identify up to five characteristic frequencies, and a Gauss–Markov model was used to compute the least-squares solution for both linear and nonlinear components simultaneously.

All PPP coordinates obtained from shorter observation sessions were then compared with the reference models by computing residuals, hereafter referred to as "real errors" ( $\delta_{err}$) (Fig. 3b).

Finally, the real errors were compared with the formal errors expressed in the covariance matrix of each solution. This step is particularly relevant for applications where each benchmark is surveyed only once and no geometric redundancy is available, as in network-based approaches using multiple baselines. In such cases, the formal error provided by the software is the only indicator of coordinate quality. Therefore, assessing the reliability of this parameter is as important as analyzing the real errors themselves.

## Results

Test results are presented starting from the statistical analysis of the real errors $\delta_{err}$, providing indications on the repeatability of the coordinates depending on the observing-session time span and the considered GNSS constellations. Then, a discussion on the reliability of the PRIDE PPP-AR formal errors is provided together with indications on how to practically use it.

### Precision vs. time

The time series of the real errors $\delta_{err}$ (residuals to the reference position models) present some few outliers, mainly concentrated in solutions obtained from short observing sessions. We discarded such outliers from the statistics presented in this section by setting a 20 cm threshold. The choice considers that, for instance, over the next years such accuracy will be formally provided by the Galileo HAS (Naciri et al. 2023) service, making useless any PPP post-processed solution for applications requiring lower precisions. Figure 4 resume the percentage of outlier positions detected for each observation time span over the 9 globally distributed stations.

Rejection percentages for time spans above three hours are all zero, thus not reported in the figure. Considering the full constellations GNSS solutions, for time spans at least one hour long the percentage of solutions with errors above 20 cm can be considered negligible, being always below 0.4%, with the only exception of the one hour solutions from the PIE1 station. Statistics rise for the half an hour PPP solutions, but mostly remain within 2%, again with the only exception of the PIE1 station showing rejection rates form 7.7% to about 18.7%. A detailed analysis shown that PIE1 site is affected by significantly high cycle-slip rate, particularly for BeiDou and Glonass constellations, probably due to the presence of a VLBI (Very Long Baseline Interferometry) antenna nearby the station. As for GPS only solutions, the percentage of outliers are just slightly higher than multi-GNSS ones, whereas Galileo shows significant percentages for one hour and half an hour solutions, especially on the East and Up components. Using GPS or Galileo only, the PIE1 station does not show the biased behavior shown using full constellations, deriving from Glonass and BeiDou data.

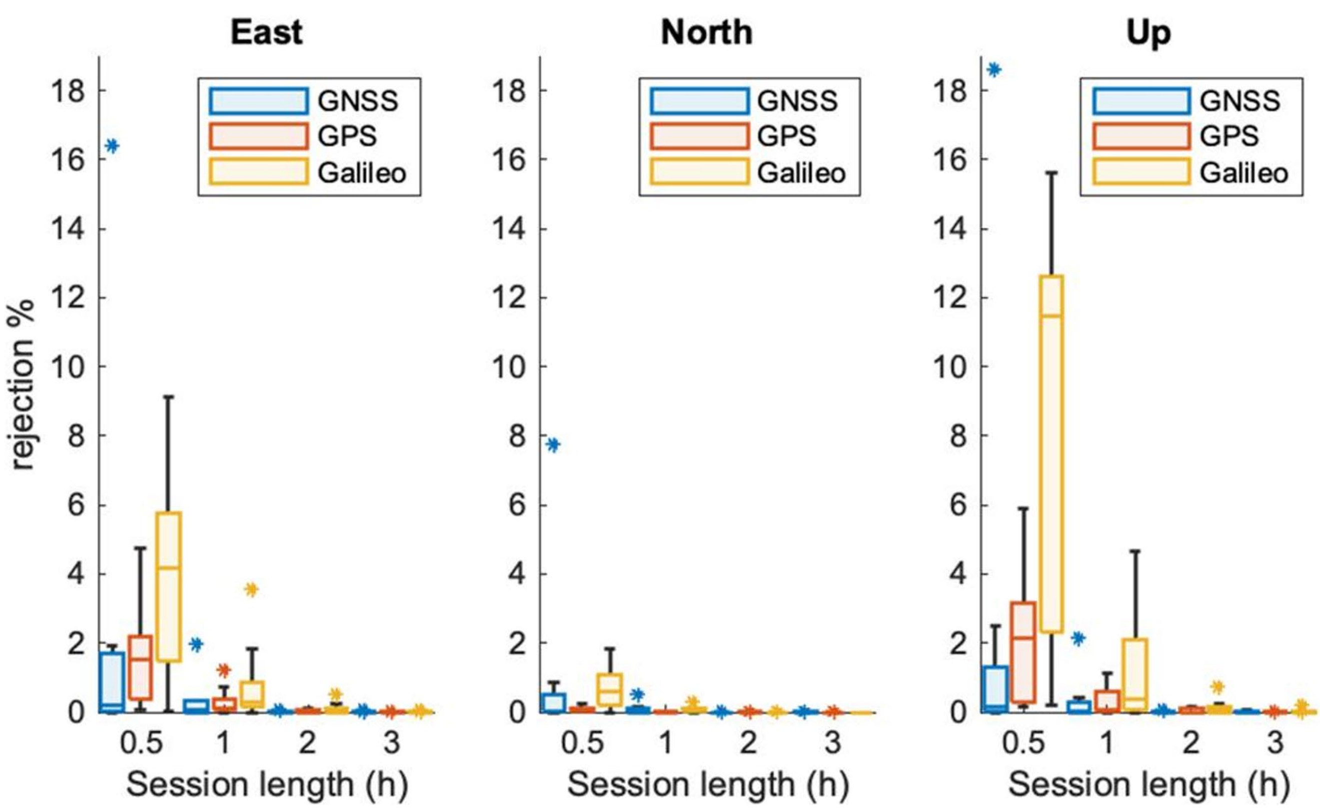


**Fig. 4** Boxplot showing statistics of rejected solutions for the nine IGS GNSS stations. Rejected coordinates have real error $\delta_{err}$ larger than 20 cm. Boxes indicate interquartile ranges, whiskers represent extreme values, and asterisks denote outliers. GNSS results refer to full-constellations data

In general, the solutions above 20 cm of error are mainly detectable looking at the Up and Easting components, while the Northing one is more accurate.

Once excluded the outlier solutions from the dataset, for each site and each time span the standard deviation of the errors was computed. Figure 5 reports the statistics on these standard deviations computed on the 9 stations of the global dataset.

The precision of PRIDE PPP-AR for long observing sessions (12–24 h) is at the mm level considering multi-GNSS observations: less than 3 mm (1σ) in the plane directions and about 7 mm in height. As for the shorter observations, half an hour data leads to precision mostly within 2 cm and 3 cm in the horizontal and vertical directions respectively. For a few stations the error 1σ is up to 4 cm. Moving from half an hour to two hours of data acquisition the errors decrease significantly, down to 1 cm for plane components and 2 cm along the Up in almost all cases. From 3 to 6 h precisions slightly improve. Overall, errors along the northing direction are smaller than the Easting and Up ones when considering shorter observations.

For GPS-only and Galileo-only solutions, precision decreases notably compared with multi-GNSS, particularly for shorter sessions. For example, Galileo 1σ errors are nearly twice those of GNSS for one-hour or shorter sessions. However, results vary strongly among sites at THU2, Galileo performance is nearly comparable to multi-GNSS. GPS precision generally lies between GNSS and Galileo values. By comparing GPS results to those obtained almost ten years ago by Gandolfi et al. (2017) by using the GIPSY-OASIS II software package, PRIDE PPP-AR performance have improved about 30% considering the observations spans of on hour or less, whereas for 3 h sessions very similar precisions were found. Such improvements on shorter sessions could comes from the different and up to date PPP algorithm that PRIDE PPP-AR implements and from improvements in the computation of GPS products.

zFinally, to provide more practical insights on the positioning performance of a short time static survey for PPP processing, Fig. 6 shows the percentage of residuals above a certain threshold $\delta_{th}$ depending on the observation time span. These results come from GNSS data of the globally distributed network, having excluded the PIE1 station which shown outlier behavior. As for the plane directions, half an hour acquisitions are enough to have a 1 cm level precision in about 95% of the cases and 5 cm in more than 98%. To guarantee errors below 1 cm in more than 98% of cases, 2 h acquisitions are necessary, while only using 12 h of data such percentage drops below 1%. Nevertheless, 3 cm level of precision could be achieved with about 99.5%

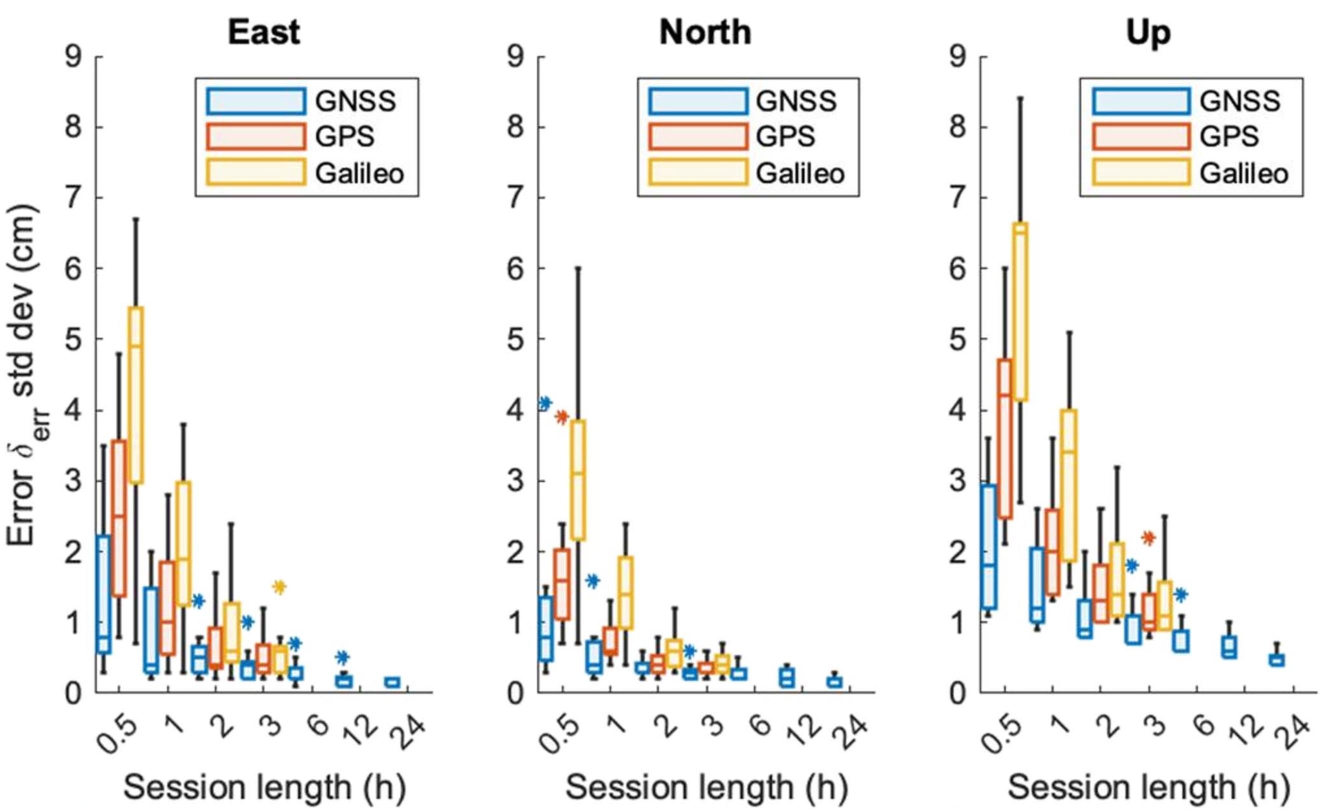


**Fig. 5** Boxplot showing statistics of the standard deviations of real errors ( $\delta_{err}$) across the 9 GNSS station from the IGS network. Boxes indicate interquartile ranges, whiskers represent extreme values, and asterisks denote outliers. GNSS results refer to full-constellations data

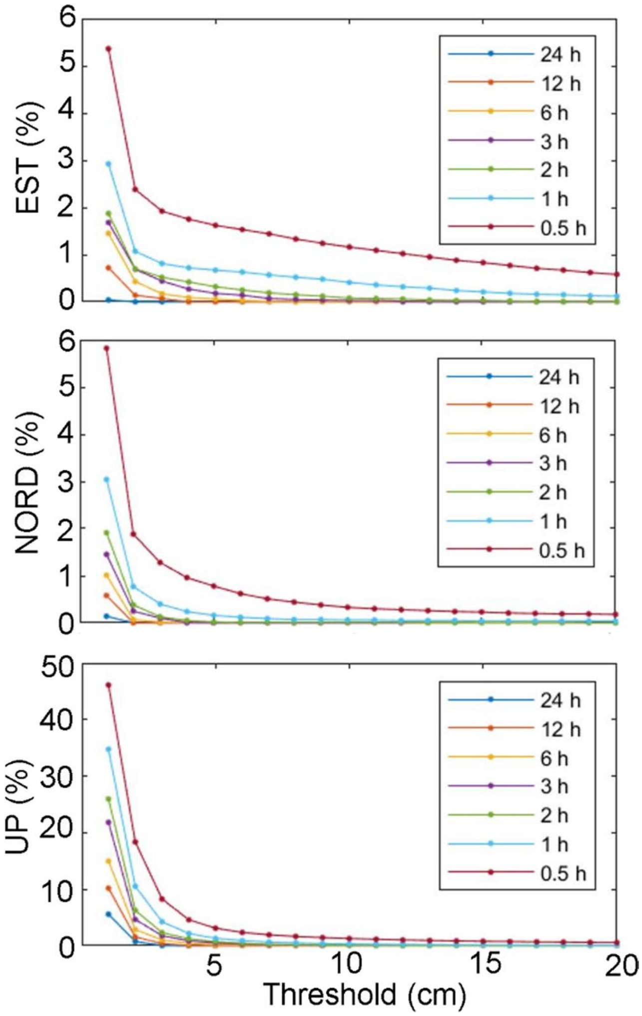


**Fig. 6** Graphs showing the percentage of PPP solutions with errors $\delta_{err}$ exceeding thresholds on the x-axis. Colors indicate observation duration

probability using two hours acquisitions. In general, precisions on Northing direction are higher than along East for the shorter observation spans.

Vertical errors are higher and, for instance, half an hour observations lead to 5% error above 4 cm. Roughly, to work with enough confidence (97.5%) within 3 cm of error, at least 3 h observations are necessary, while 6 h are required if the goal is the 2 cm height precision.

A complementary analysis was performed using the 30-day dataset from three Italian stations. The goal was to evaluate the impact of 1 Hz data versus 30-second sampling for short sessions. The difference was found to be negligible: for GNSS data, discrepancies in the standard deviation of residuals were below 1 mm, while for GPS or Galileo only, they reached up to 4–6 mm. In these cases, 30-second data yielded slightly better precision than 1 Hz data, particularly for 30-minute and one-hour sessions. This may result from oversampling effects (i.e. many numerical inputs, but highly correlated) that negatively impact PPP processing when geometric redundancy is low since satellites positions do not vary significantly over short periods. Table 2 summarizes the mean standard deviations (1σ) of the real errors $\delta_{err}$, averaged over the three Italian stations (Fig. 1b). These results are consistent with those obtained from the nine IGS stations for full-GNSS and Galileo-only solutions. However, for the 1 h and 0.5 h sessions, GPS errors over the Italian stations were larger than Galileo, contrary to the trend observed for the global network.

## Reliability of the formal error

The formal error provided by PRIDE PPP-AR for each solution was considered with the aim of verifying its usability to have insights on the actual quality of the computed coordinates. This would be useful to surveyors performing single session of GNSS data acquisition for PPP, thus without any geometrical redundancy. The software actually provides a cofactor matrix representing the intrinsic precision of the unknown parameters as it comes from the weighting of the observables in the data processing. Thus, such information is not intended to directly estimate the actual coordinates accuracy.

The matrix of each solution was transformed into a full-covariance matrix and then rotated to express uncertainties along the topocentric directions ENU. First, the cross-correlation coefficients between the time series of the errors ($\delta_{err}$) and those of the estimated standard deviations ($\sigma_{Pride}$), namely the square roots of the diagonal elements of each covariance matrix, were computed. Such

**Table 2** Standard deviations of the real errors $\delta_{err}$ averaged over the 3 GNSS permanent stations located in Italy (Fig. 1b), expressed in cm

| | mean σ (cm) | | | | | | | | |
|---|---|---|---|---|---|---|---|---|---|
| | Multi-GNSS | | | GPS | | | Galileo | | |
| Session length | *N* | *E* | *U* | *N* | *E* | *U* | *N* | *E* | *U* |
| *3 h* | 0.3 | 0.3 | 1.0 | 0.5 | 0.7 | 1.6 | 0.5 | 0.7 | 1.1 |
| *2 h* | 0.3 | 0.3 | 1.3 | 0.5 | 0.8 | 1.7 | 0.8 | 0.6 | 1.3 |
| *1 h* | 0.4 | 0.4 | 1.4 | 2.0 | 3.0 | 4.0 | 1.8 | 2.6 | 2.8 |
| *0.5 h* | 0.6 | 0.6 | 2.0 | 4.7 | 6.1 | 7.0 | 4.2 | 5.5 | 5.5 |

cross-correlations range between 0.6 and 0.7 depending on the observation time span considered, with a variability of 0–0.2.2 standard deviation depending on the site. Nevertheless, the formal error given by the software shown to be largely underrated. Therefore, an attempt to estimate Scale Factors (SFs) to be applied to $\sigma_{Pride}$ to make it usable was pursued.

This was done testing iteratively several SF values, also considering a threshold value for the coordinates error $\delta_{th}$ and the probability to commit type I or type II errors using the scaled formal error $\sigma_{SF} = \sigma_{Pride}*SF$ to assess the solution' quality. The $\delta_{th}$ value should be related to the goals of the survey and its expected accuracy, while errors were considered by defining them as:

- Type I error ($E_I$): accepting coordinates affected by a too big error, so that $\begin{cases} \sigma_{SF} \leq \delta_{th} \\ \delta_{err} \geq \delta_{th} \end{cases}$;
- Type II error ($E_{II}$): rejecting coordinates with acceptable error, so that $\begin{cases} \sigma_{SF} \geq \delta_{th} \\ \delta_{err} \leq \delta_{th} \end{cases}$;

SFs ranging from 1 to 500 were tested. It was found that results in terms of $E_I$ and $E_{II}$ highly depend on both the selected $\delta_{th}$ threshold and the observation time span. Moreover, error estimates are in a different relation with the real errors dependig on the considered direction: North, East or Up. Therefore, ad hoc SFs were computed for each time span and each coordinate component considering different error thresholds. Such scale factors were selected by minimizing the combined probability of occurring in errors $E_I$ or $E_{II}$. Since accepting and using wrong coordinates ($E_I$) is in practice more dangerous than rejecting a good measurement ($E_{II}$), the error probability to be minimized was actually the combination $E_c = E_I * 0.75 + E_{II} * 0.25$.

The PIE1 data were not considered in the estimation of the SFs to prevent the results be affected by site-dependent biases. Nevertheless, the proposed values refer to antennas working in good sky visibility and limited multipath. Therefore, the here computed SFs might not work at best for surveys performed under less favorable environmental conditions.

Results are reported in Figs. 7, 8 and 9 by considering three different scenarios.

**Case 1** $\delta_{th,\,North} = \delta_{th,\,East} = 1cm, \quad \delta_{th,Up} = 2cm.$ This scenario considers the most demanding case of reference frame densification as, for instance, the definition of a passive network of benchmark in a remote area, the setting of benchmarks for high precision land survey to be performed through total stations or, differently, the case of monitoring of a wide and remote unstable area.

**Case 2** $\delta_{th,\,North} = \delta_{th,\,East} = 3cm, \quad \delta_{th,Up} = 5cm.$ This scenario is similar to Case 1, considering less demanding accuracies or a lower sensitivity to displacements.

**Case 3** $\delta_{th,\,North} = \delta_{th,\,East} = \delta_{th,Up} = 10cm$This scenario considers, for instance, the measurement of GCP for airborne photogrammetry or Lidar surveys in remote areas.

Figures 7 and 8-9 show the scale factors (blue bins) and the related $E_c$ error probability (Orange lines) obtained for Case 1, Case 2 and Case 3 respectively, depending on the observing session time spans. It worth noting that $E_c$ does not represent the probability to have coordinates' errors higher than $\delta_{th}$, but instead it means the probability of wrongly accept or discard such coordinates after checking the formal error $\sigma_{SF}$. Results for data acquisition of 12 h and 24 h are not reported since for the given requirements ($\delta_{th}$ values) the error probabilities are zeros or negliegible (minor than 0.2%) even in the most demanding case just considering $\sigma_{Pride}$ values. Moreover, measuring sessions of 12 h or more are less likely doable in the surveying practice.

As for Case 1, for instance, considering plane components and applying the here defined SFs to the PPP formal errors $\sigma_{Pride}$ it would be possible to perform a survey compliant to the precision requirements with less than 1% probability to wrongly use the computed coordinates by acquiring at least 2 h of data. Nevertheless, by using half an hour acquisitions the $E_c$ probability for Northing and Easting coordinates is about 2%. As for the hight, to limit the error probability within 5% at least one hour data should be acquired, increasing to 6 h or more to have $E_c$ lower than 1%.

In Case 2 scenario some larger scale factor should be applied to the PPP formal errors, thus obtaining $E_c$ probabilities about 0.5% and 1% for plane and height components respectively using just half a hour data records, while one hour is enough to drop such error probabilities to 0.2% and 0.5%. For observing sessions 6 h long, the error probabilities are almost negligible.

Figure 9 relates to Case 3 and shows that, once properly scaled, the PPP formal error is highly reliable ($E_c$ within 0.5%) also for the shorter observing sessions. Still, moving to 2 h surveys or longer actually makes the probability of misinterpreting the coordinates quality negligible, meaning $E_c$ lower than 0.1% also for the height component.

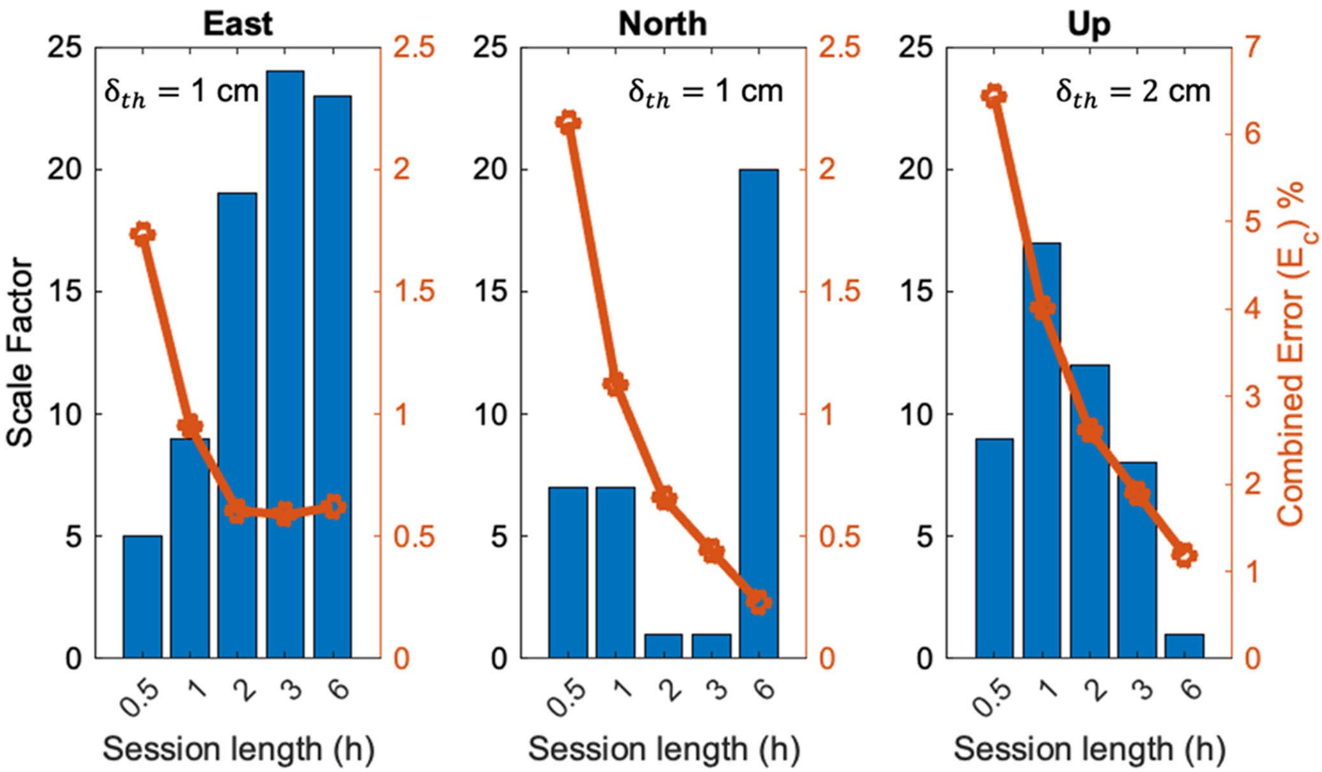


**Fig. 7** Reliability of the scaled formal error $\sigma_{SF}$ for Case 1 scenario. Blue bars show the computed scale factors minimizing the combined error ($E_c$); red dots represent corresponding $E_c$ values

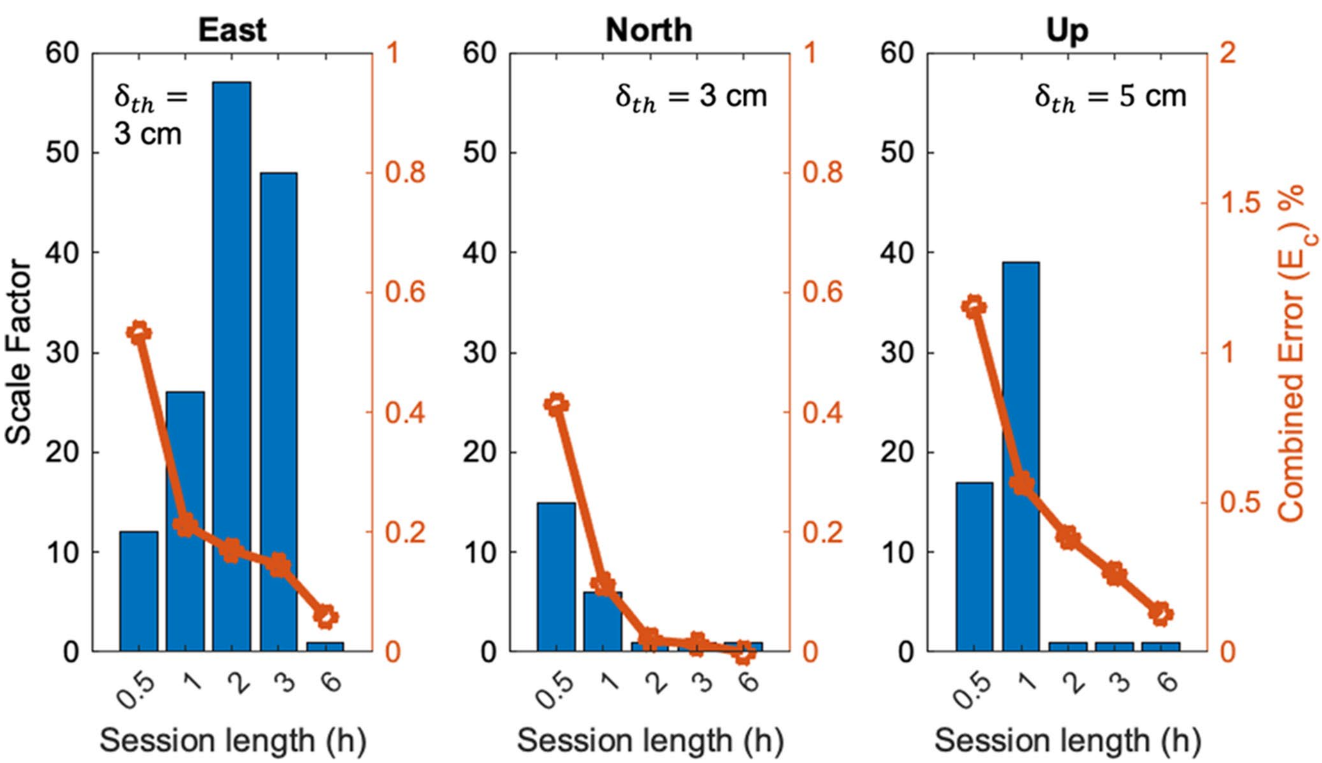


**Fig. 8** Reliability of scaled formal error $\sigma_{SF}$ for Case 2. Blue bars show scale factors minimizing $E_c$; red dots represent resulting $E_c$ values

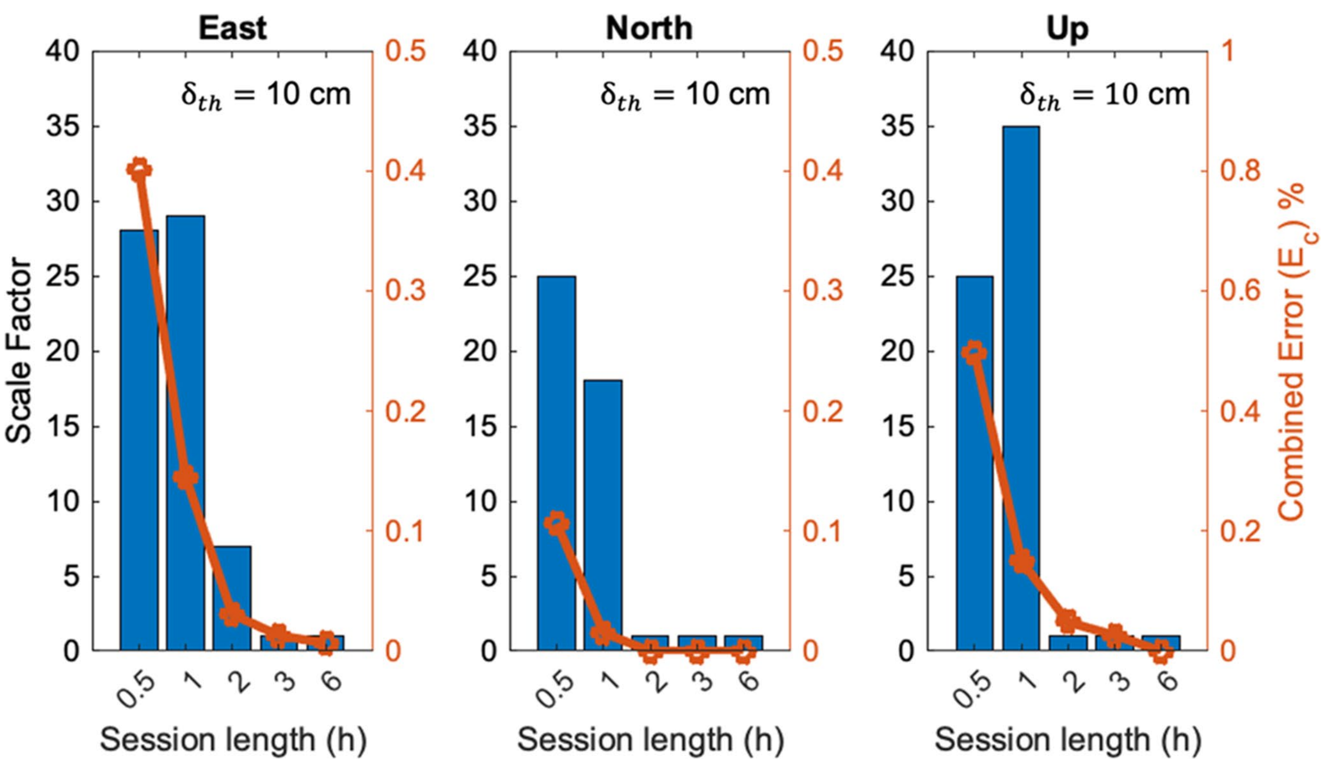


**Fig. 9** Reliability of scaled formal error $\sigma_{SF}$ for Case 3. Blue bars show scale factors minimizing $E_c$; red dots represent resulting $E_c$ values

## Conclusions

This study investigated the use of the free PRIDE PPP-AR software package for GNSS surveys that require observation sessions as short as possible to remain feasible or productive. A large dataset comprising one year of daily data from nine IGS stations was used, each divided into different time spans to simulate shorter observation sessions. Time spans of 12, 6, 3, 2, 1, and 0.5 h were tested.

Daily PPP solutions were used to build nonlinear position models serving as references for the coordinates obtained from each simulated survey. Reliable and robust statistics describing the actual precision of PPP processing as a function of input data length were derived by analyzing coordinate residuals with respect to the reference models. Moreover, since PPP surveys inherently lack geometric redundancy (i.e., multiple baselines converging on the same point), surveyors have no direct means to evaluate the quality of their results without repeating the survey. Therefore, the reliability of the formal errors provided by PRIDE PPP-AR was also examined. The software was found to produce formal errors that are largely underestimated and not representative of the true positioning quality. Consequently, a possible method to exploit these formal errors, by applying suitable scale factors to assess coordinate reliability, is proposed.

For example, in full-constellation GNSS surveys with two-hour observation sessions, PRIDE PPP-AR achieves horizontal positioning errors within 1 cm in about 98% of cases, with only a 0.5% probability of misjudging coordinate quality when using the scaled formal errors. If a precision requirement of 3 cm is acceptable, observation sessions of just 30 min can yield similar reliability. Vertical components are less precise, and a more realistic target for short sessions is 5 cm accuracy, achievable with 2–3 h observations. As shown in Figs. 6 and 9, 30 min observations are more likely to be suitable when the 3D accuracy requirements are within 10 cm. The paper provides graphs useful for planning surveys according to the required precision and reliability levels. Overall, two-hour observation sessions appear to offer the most effective trade-off between time and positioning performance when using PRIDE PPP-AR.

A comparison between full-GNSS and single-constellation (GPS-only or Galileo-only) solutions was also performed. Single-constellation results are less precise, particularly for observation sessions shorter than 3 h. In such cases, positioning errors from Galileo data are nearly double those from full-GNSS solutions, while GPS data yield intermediate performance.

Analysis by site location confirmed lower precision at equatorial latitudes, in agreement with Kurtz et al. (2024). Specifically, for observation sessions shorter than six hours, positioning precision is about 50% worse at low latitudes than at mid- and high-latitude stations. Finally, using a 1 Hz sampling rate instead of 30-second sampling did not improve positioning performance. On the contrary, for 1 h session or shorter, higher sampling rates slightly degraded precision in the case of GPS-only or Galileo-only data, likely due to oversampling effects.

Although online PPP services could in principle be used by technicians for similar applications, PRIDE PPP-AR offers a practical alternative, as it can be easily installed in a user-friendly GUI version and run without limitations on the amount of input data. Moreover, this paper provides comprehensive insights on the precision achievable with the software using standard parameters, and proposes a method to interpret the estimated errors for a reliable assessment of result quality.

**Author contributions** All authors contributed to the study conception and design. Cappuccio M. reorganized the data and performed the PRIDE PPP-AR processing. Tavasci L. supervised the PPP processing, provided guidelines for the post-processing strategy and analyzed the results. Luca P. and Gandolfi S. supervised both the computations and the paper writing. The first draft of the manuscript was written by Tavasci L. All authors read, commented and approved the final manuscript.

**Funding** Open access funding provided by Alma Mater Studiorum - Università di Bologna within the CRUI-CARE Agreement. The authors did not receive support from any organization for the submitted work.

**Data availability** The data on which this research is based are available from the corresponding author exclusively for fully justified scientific purposes.

## Declarations

**Competing interests** The authors declare no competing interests.



## References

Abou-Galala M, Rabah M, Kaloop M, Zidan ZM (2018) Assessment of the accuracy and convergence period of precise point positioning. Alexandria Eng J 57(3):1721–1726. https://doi.org/10.1016/j.aej.2017.04.019

An X, Meng X, Jiang W (2020) Multi-constellation GNSS precise point positioning with multi-frequency raw observations and dual-frequency observations of ionospheric-free linear combination. Satell Navig 1(1):7. https://doi.org/10.1186/s43020-020-0009-x

Atiz OF, Shakor AQ, Ogutcu S, Alcay S (2023) Performance investigation of trimble RTX correction service with multi-GNSS constellation. Surv Rev 55(388):44–54. https://doi.org/10.1080/00396265.2021.1999128

Barbarella M, Gandolfi S, Poluzzi L, Tavasci L (2018) Precision of PPP as a function of the observing-session duration. IEEE Trans Aerosp Electron Syst 54(6):2827–2836. https://doi.org/10.1109/TAES.2018.2831098

Bertiger W, Desai SD, Haines B, Harvey N, Moore AW, Owen S, Weiss JP (2010) Single receiver phase ambiguity resolution with GPS data. J Geod 84(5):327–337. https://doi.org/10.1007/s00190-010-0371-9

Bertiger W, Bar-Sever Y, Dorsey A, Haines B, Harvey N, Hemberger D, Heflin M, Lu W, Miller M, Moore AW, Murphy D, Ries P, Romans L, Sibois A, Sibthorpe A, Szilagyi B, Vallisneri M, Willis P (2020) GipsyX/RTGx, a new tool set for space geodetic operations and research. Adv Space Res 66(3):469–489. https://doi.org/10.1016/j.asr.2020.04.015

C-nav positioning solutions. (n.d.). Retrieved February 7, 2025, from https://www.oceaneering.com/positioning-solutions/

Cappuccio M, Tavasci L, Vecchi E, Frezzotti M, Gandolfi S (2024) A PPP kinematic application on historical GPS data: the reprocessing of the ITASE98-99 Antarctica mission height profiles. GPS Solut 28(3):120. https://doi.org/10.1007/s10291-024-01660-4

Chu F-Y, Yang M (2014) GPS/Galileo long baseline computation: method and performance analyses. GPS Solut 18(2):263–272. https://doi.org/10.1007/s10291-013-0327-7

Dach R, Lutz S, Walser P, Fridez P (2015) BerneseGNSS Software Version 5.2. https://doi.org/10.7892/boris.72297

Dach R, Schaer S, Arnold D, Brockmann E, Kalarus MS, Lasser M, Stebler P, Jäggi A (2024) CODE final product series for the IGS. https://doi.org/10.48350/197025

Gandolfi S, Tavasci L, Poluzzi L (2017) Study on GPS–PPP precision for short observation sessions. GPS Solut 21(3):887–896. https://doi.org/10.1007/s10291-016-0575-4

Geng J, Chen X, Pan Y, Mao S, Li C, Zhou J, Zhang K (2019) PRIDE PPP-AR: an open-source software for GPS PPP ambiguity resolution. GPS Solut 23(4):91. https://doi.org/10.1007/s10291-019-0888-1

Glaner M, Weber R (2021) PPP with integer ambiguity resolution for GPS and Galileo using satellite products from different analysis centers. GPS Solut 25(3):102. https://doi.org/10.1007/s10291-021-01140-z

Guo J, Xu X, Zhao Q, Liu J (2016) Precise orbit determination for quad-constellation satellites at Wuhan university: strategy, result validation, and comparison. J Geod 90(2):143–159. https://doi.org/10.1007/s00190-015-0862-9

Jianghui Geng X, Meng AH, Dodson, Felix N, Teferle (2010) Integer ambiguity resolution in precise point positioning: method comparison. J Geodesy 84:569–581

JONGEPDE, & TIBERIUSC (1996) The LAMBDA method for integer ambiguity Estimation. In Delft Geodetic Computing Center LGR

Kouba J, Héroux P (2001) Precise point positioning using IGS orbit and clock products. GPS Solut 5(2):12–28. https://doi.org/10.1007/PL00012883

Kouba J, Lahaye F, Tétreault P (2017) Precise Point Positioning. In Springer Handbook of Global Navigation Satellite Systems (pp. 723–751). Springer International Publishing. https://doi.org/10.1007/978-3-319-42928-1_25

Kurtz BM, Gómez DD, Bevis MG (2024) Characterization of the precision of PPP solutions as a function of latitude and session length. J Geodetic Sci, 14(1)

Leandro Rodrigo F, Marcelo C, Santos, Richard B, Langley (2007) GAPS: The GPS analysis and positioning software-A brief overview. Proceedings of the 20th International Technical Meeting of the Satellite Division of The Institute of Navigation (ION GNSS 2007)

Li B, Shen Y, Feng Y, Gao W, Yang L (2014) GNSS ambiguity resolution with controllable failure rate for long baseline network RTK. J Geod 88(2):99–112. https://doi.org/10.1007/s00190-013-0670-z

Mutlu B, Erol S, Alkan RM (2023) The performance analysis of the post-mission web-based static and kinematic PPP-AR service. Rudar Geol Naftni Zb 38(4):103–116

Naciri N, Yi D, Bisnath S, de Blas FJ, Capua R (2023) Assessment of Galileo high accuracy service (HAS) test signals and preliminary positioning performance. GPS Solut 27(2):73. https://doi.org/10.1007/s10291-023-01410-y

Scargle JD (1982) Studies in astronomical time series analysis. II - statistical aspects of spectral analysis of unevenly spaced data. Astrophys J 263:835. https://doi.org/10.1086/160554

Tavasci L, Vecchi E, Gandolfi S (2021) Performance of Atlas GNSS global correction service for high-accuracy positioning. J Survey Eng. https://doi.org/10.1061/(ASCE)SU.1943-5428.0000372

Tavasci L, Lambertini A, Donati D, Girelli VA, Lattanzi G, Castellaro S, Gandolfi S, Borgatti L (2023) A laboratory for the integration of geomatic and geomechanical data: the rock pinnacle "Campanile di Val Montanaia." Remote Sens 15(19):4854. https://doi.org/10.3390/rs15194854

Teferle FN, Orliac EJ, Bingley RM (2007) An assessment of Bernese GPS software precise point positioning using IGS final products for global site velocities. GPS Solut 11(3):205–213. https://doi.org/10.1007/s10291-006-0051-7

Tetreault Pierre, Kouba Jan, Heroux Pierre, Legree Patrick (2005) CSRS-PPP: AN INTERNET SERVICE FOR GPS USER ACCESS TO THE CANADIAN SPATIAL REFERENCE FRAME. Geomatica 59(1):17–28

VanderPlas JT (2018) Understanding the Lomb–Scargle periodogram. Astrophys J Suppl Ser 236(1):16. https://doi.org/10.3847/1538-4365/aab766

Vázquez-Ontiveros JR, Padilla-Velazco J, Gaxiola-Camacho JR, Vázquez-Becerra GE (2023) Evaluation and analysis of the accuracy of Open-Source software and online services for PPP processing in static mode. Remote Sens, 15(8)

Vecchi E, Tavasci L, De Nigris N, Gandolfi S (2021) GNSS and photogrammetric UAV derived data for coastal monitoring: a case of study in Emilia-Romagna, Italy. J Mar Sci Eng 9(11):1194. https://doi.org/10.3390/jmse9111194

Webb FH, Zumberge JF (1997) An introduction to GIPSY/OASIS-II. JPL Pubblication

Yang H, He X, Ferreira V, Ji S, Xu Y, Song S (2023) Assessment of precipitable water vapor retrieved from precise point positioning with PPP-B2b service. Earth Sci Inform 16(1):315–328. https://doi.org/10.1007/s12145-023-00939-3

Zhu Y, Xing J, Li W (2023) Performance Evaluation of Atmospheric Delay Inversion by Undifferenced Uncombined Precise Point Positioning. 2023 3rd International Conference on Electronic Information Engineering and Computer Communication (EIECC), 398–401. https://doi.org/10.1109/EIECC60864.2023.10456669

Zumberge JF, Heflin MB, Jefferson DC, Watkins MM, Webb FH (1997) Precise point positioning for the efficient and robust analysis of GPS data from large networks. J Geophys Res Solid Earth 102(B3):5005–5017. https://doi.org/10.1029/96JB03860